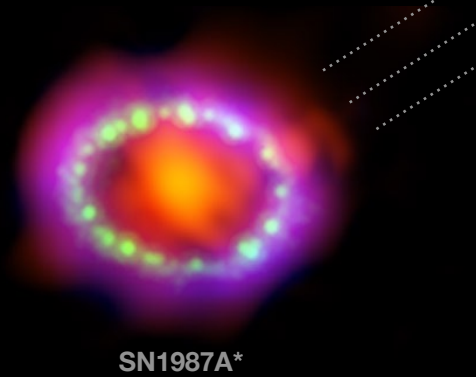


Axion-like particles and where to find them

Searching for ALPs from CCSNe with Fermi LAT's Low Energy Technique

Phys. Rev. D 104, 103001 (arXiv:2109.05790)

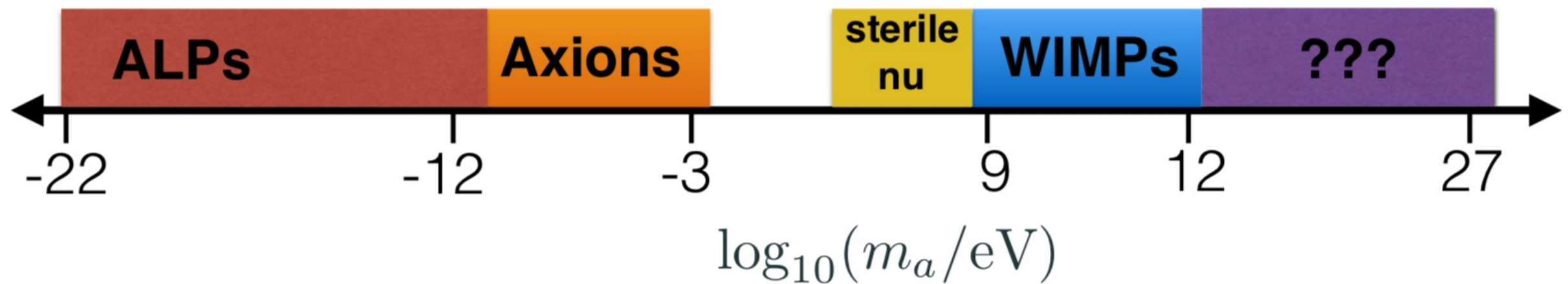


SN1987A*

Milena Crnogorčević
University of Maryland/NASA Goddard
mcrnogor@umd.edu

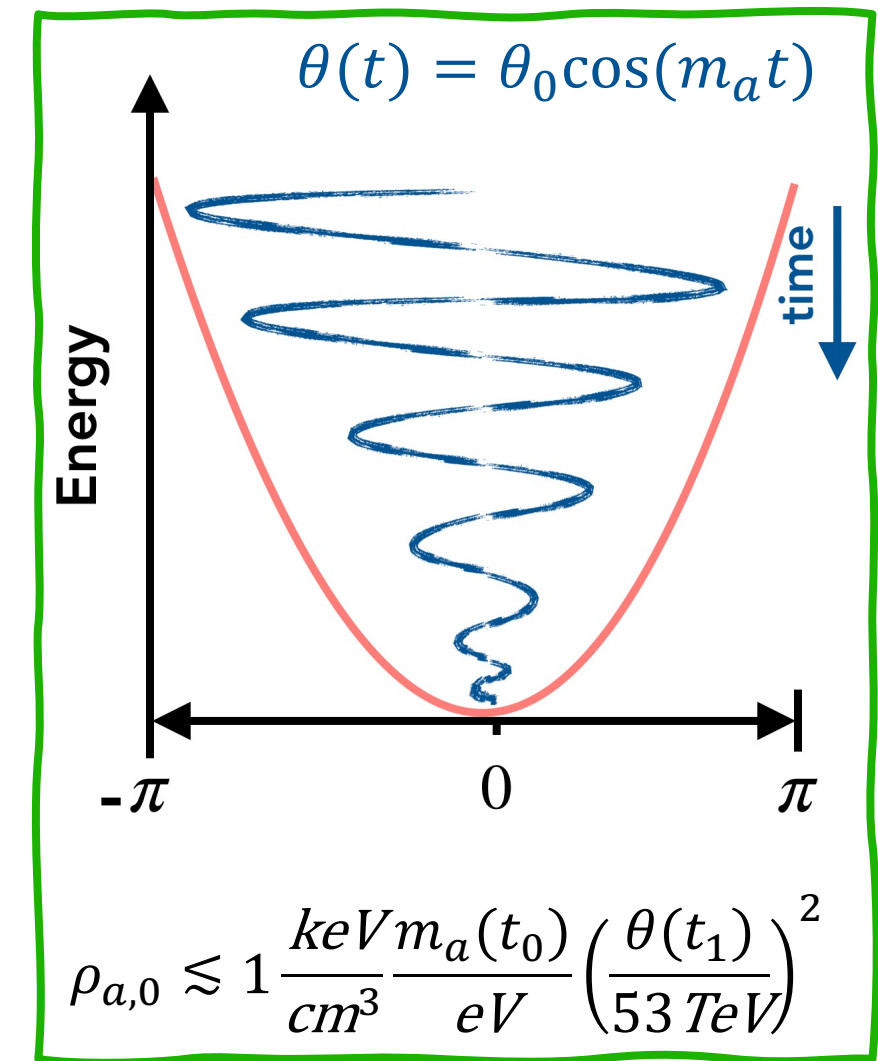
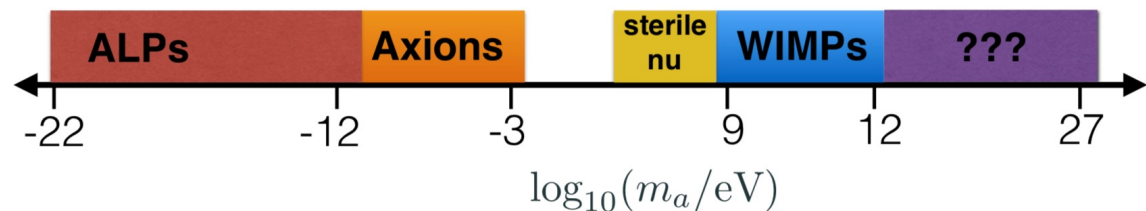
What are axion-like particles (ALPs)?

- ❖ Axion motivation: particle physics (charge-parity problem)
- ❖ WISP: weakly-interacting sub-eV particles

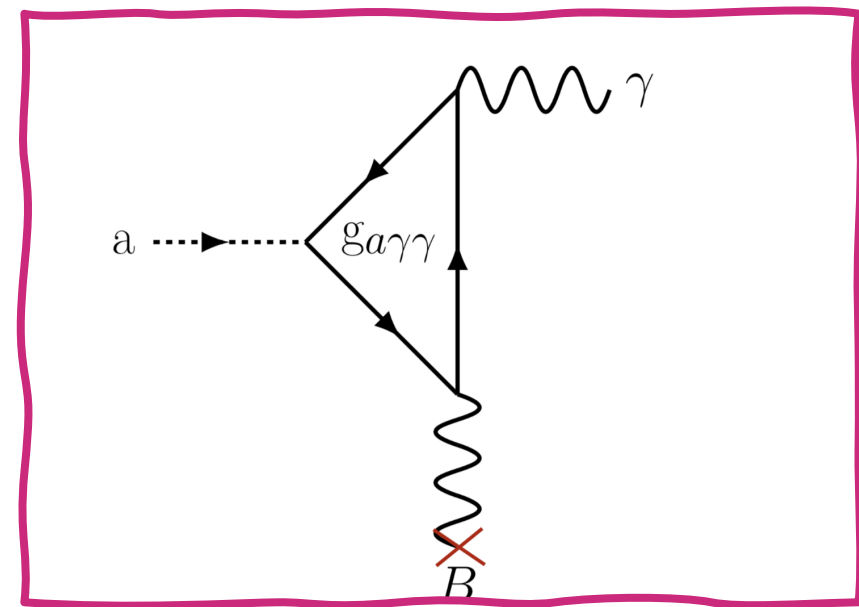


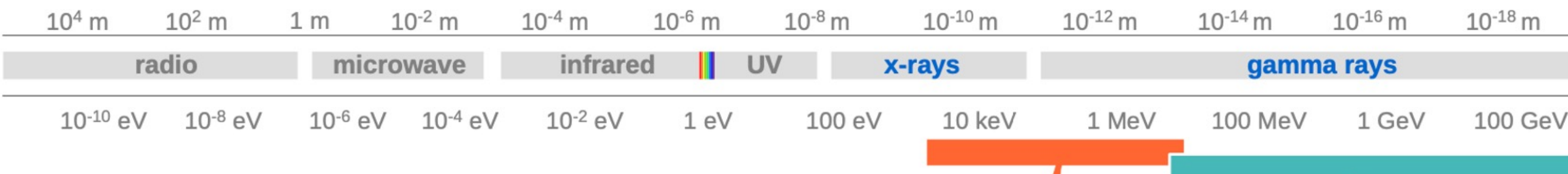
What are axion-like particles (ALPs)?

- ❖ Axion motivation: particle physics (charge-parity problem)
- ❖ WISP: weakly-interacting sub-eV particles



- ❖ Cold-matter requirements:
 - ✓ feeble interactions with SM particles
 - ✓ cosmological stability
- ❖ **Non-thermal** production of ALPs via *misalignment mechanism* or *Primakoff process*





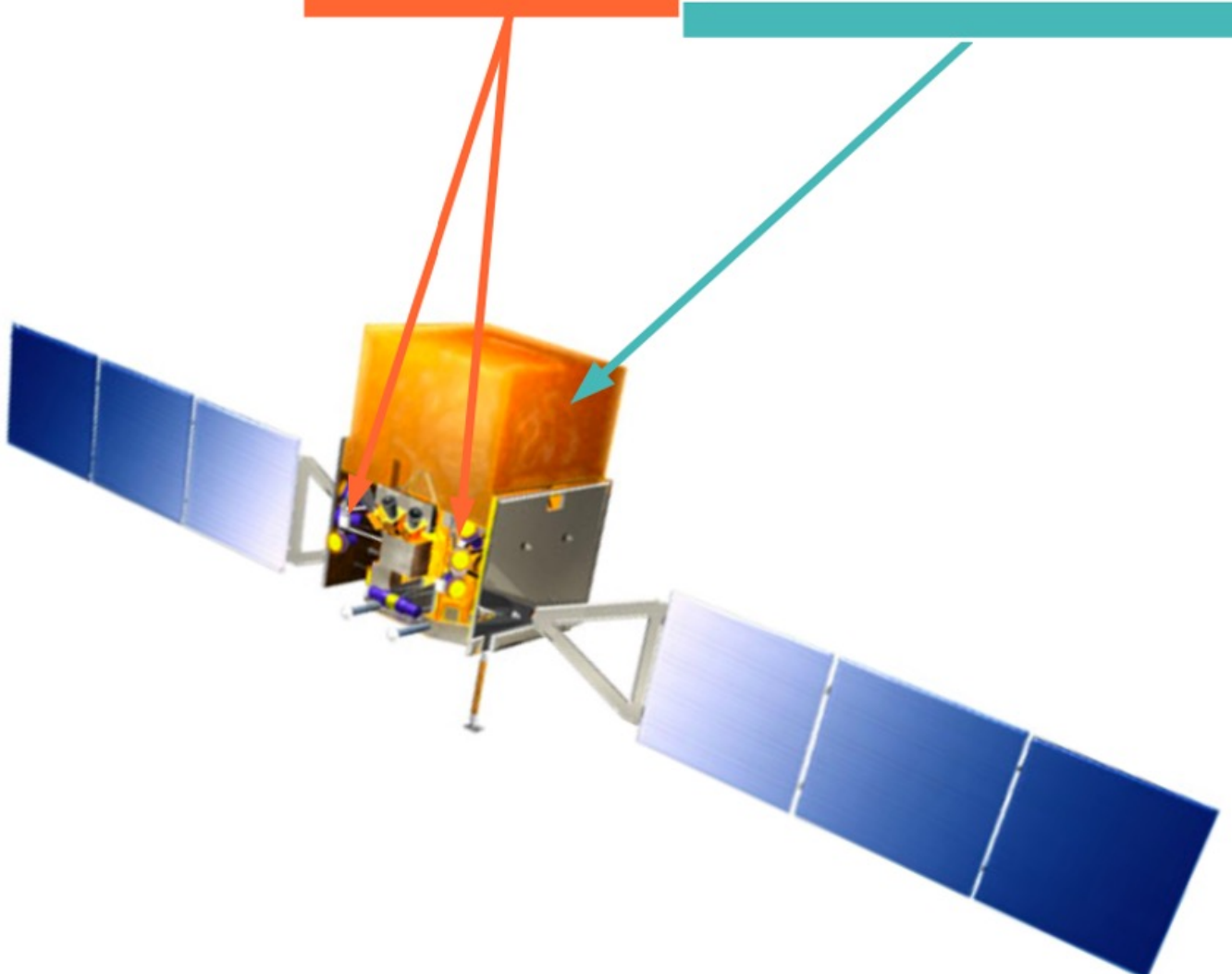
GBM Gamma-ray Burst Monitor

12 (NaI) + 2 (BGO) detectors

FoV: entire unocculted sky

8 keV to 40 MeV

~1500 bursts (~1 every day or two)



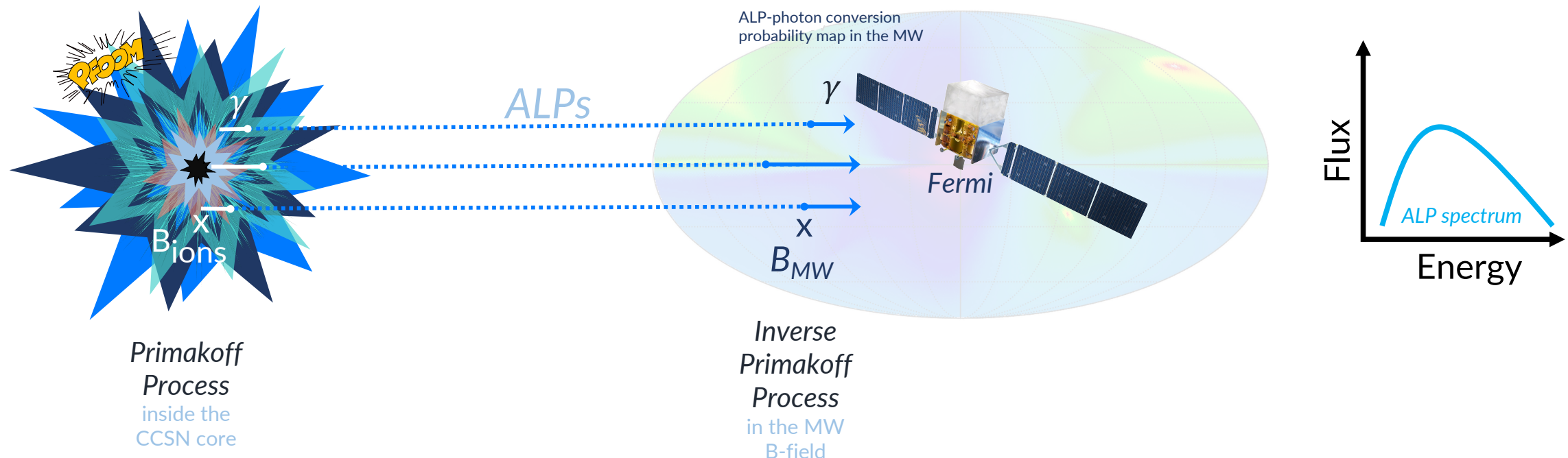
LAT Large Area Telescope

Pair-production telescope

FoV: 2.4 sr (~20% of sky)

20 MeV to >300 GeV

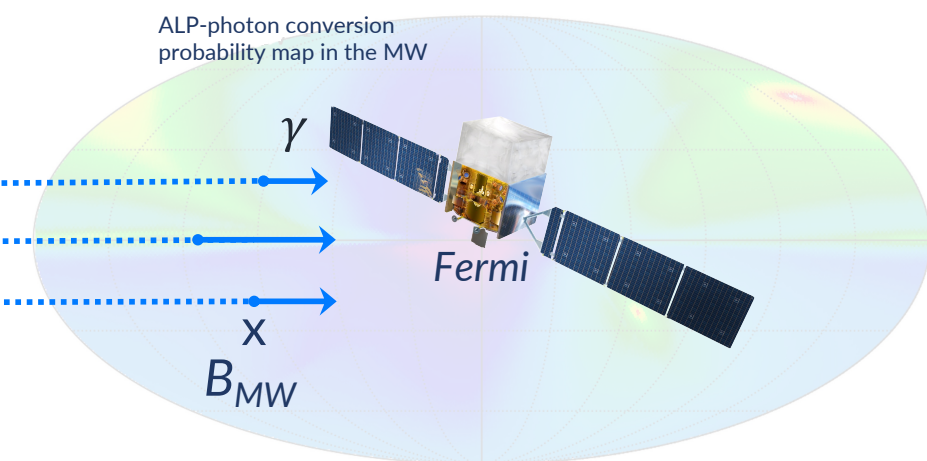
Motivation and assumptions



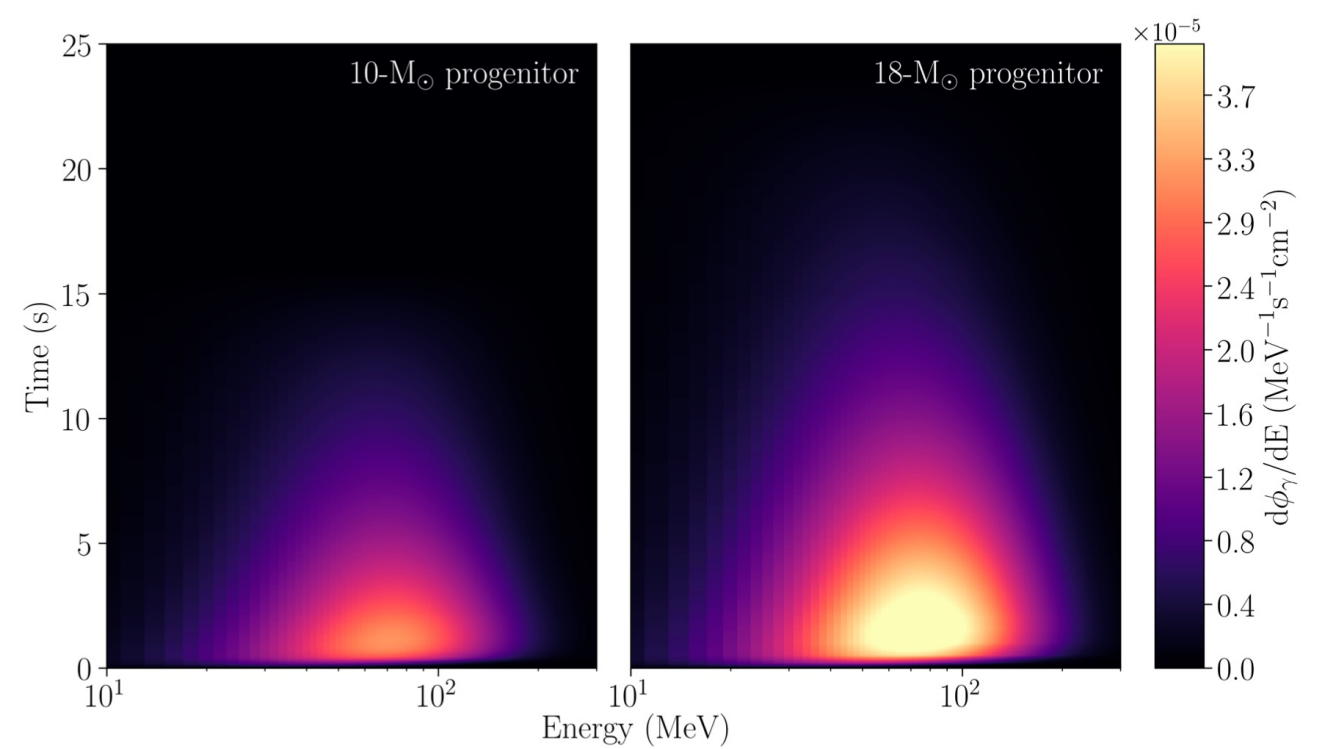
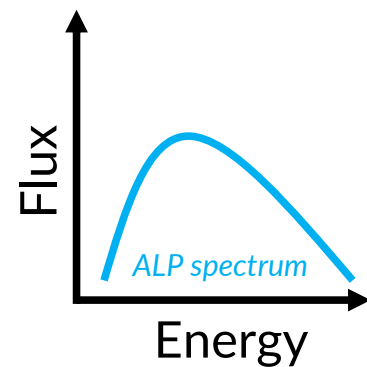
Motivation and assumptions



Primakoff
Process
inside the
CCSN core



Inverse
Primakoff
Process
in the MW
B-field

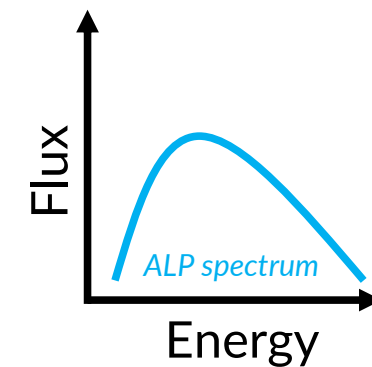
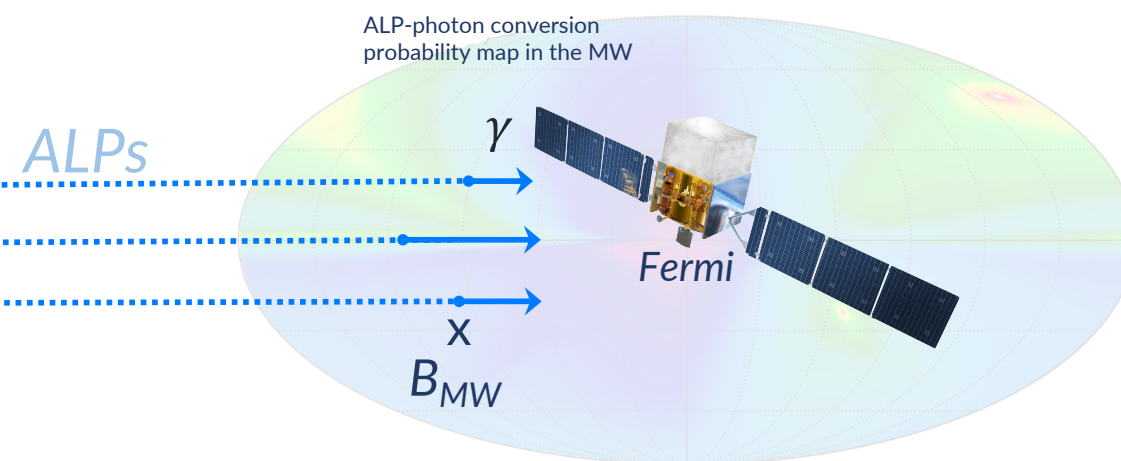


Observed evolution of the ALP-induced gamma-ray emission in time and energy in a core-collapse of a 10 and 18-M_⊙ progenitor.

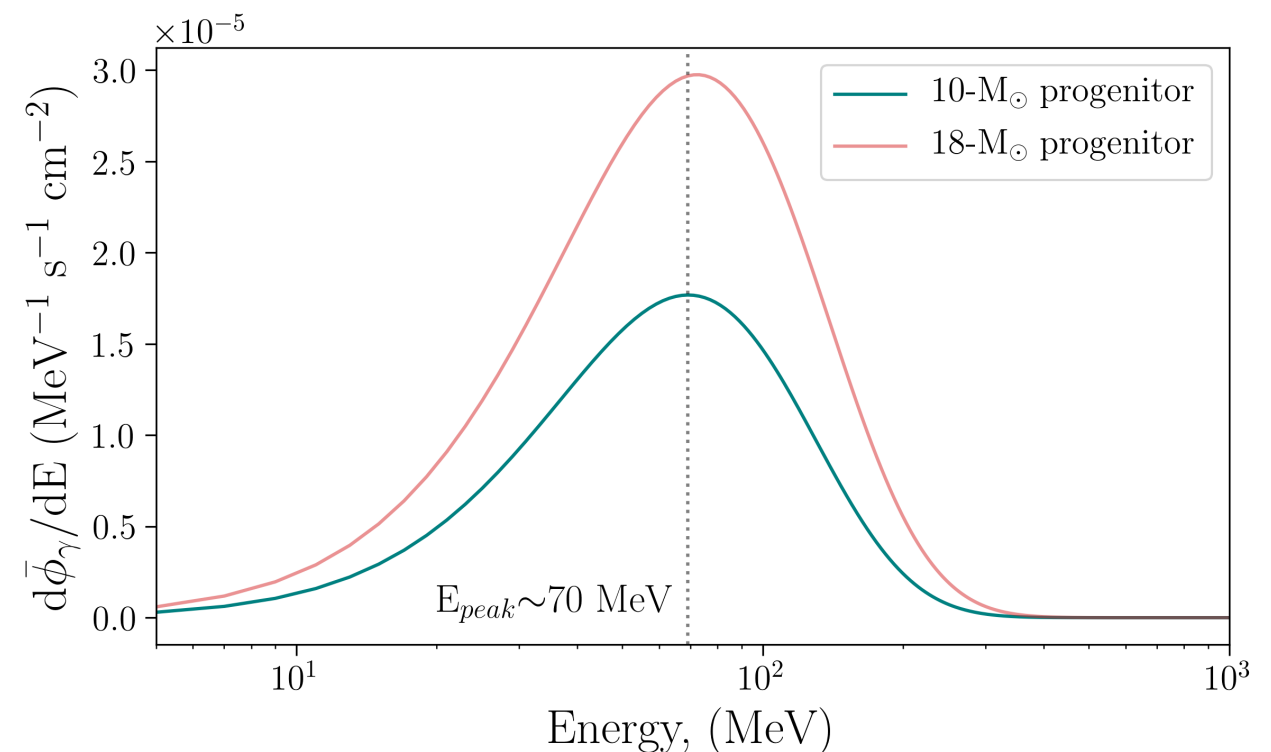
Motivation and assumptions



Primakoff
Process
inside the
CCSN core

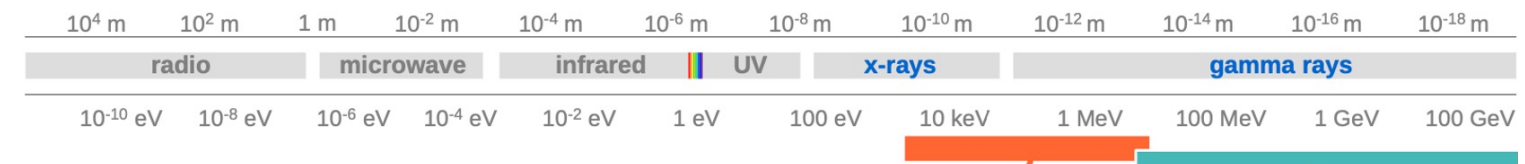
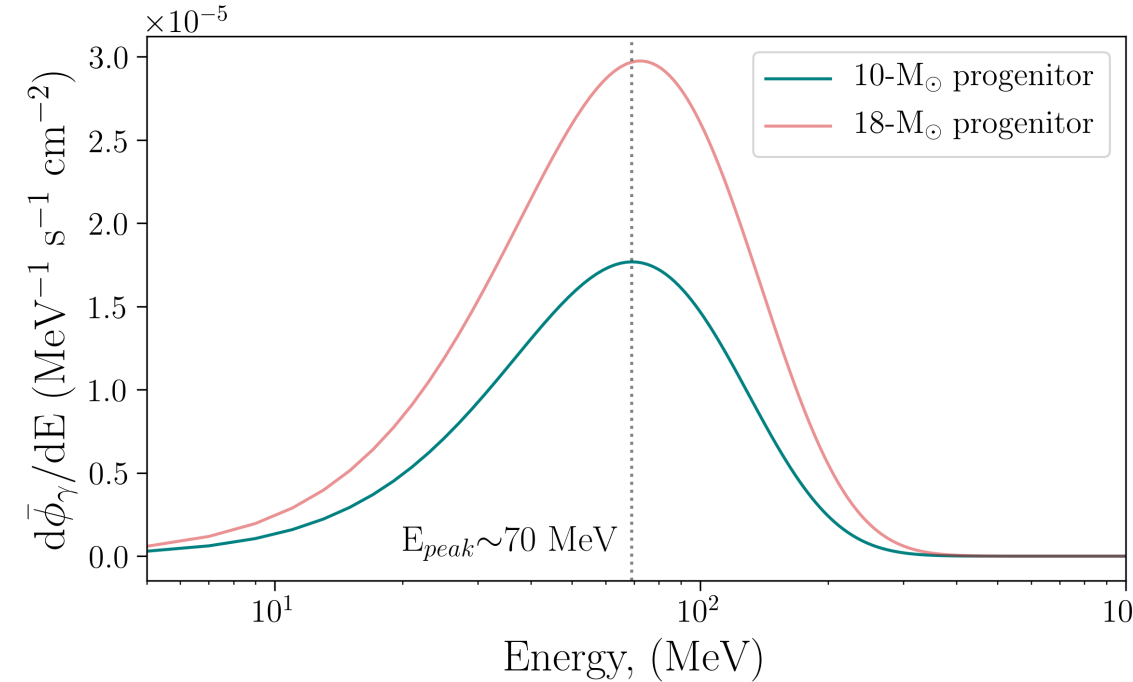


- **Motivation:** ALPs are theorized to have a unique spectral signature in the spectrum of a long GRB. No other known physical processes are predicted to produce such signature.



The observed ALP-induced gamma-ray spectrum for 10 and $18-M_\odot$ progenitors averaged over 10 seconds.

ALP spectrum



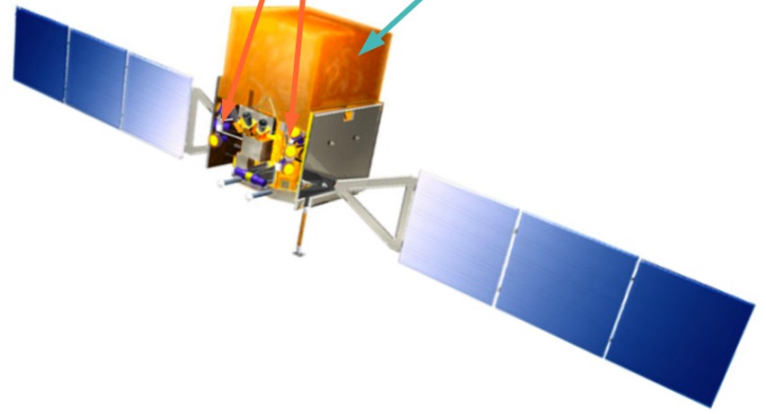
GBM Gamma-ray Burst Monitor

12 (NaI) + 2 (BGO) detectors

FoV: entire unocculted sky

8 keV to 40 MeV

~1500 bursts (~1 every day or two)



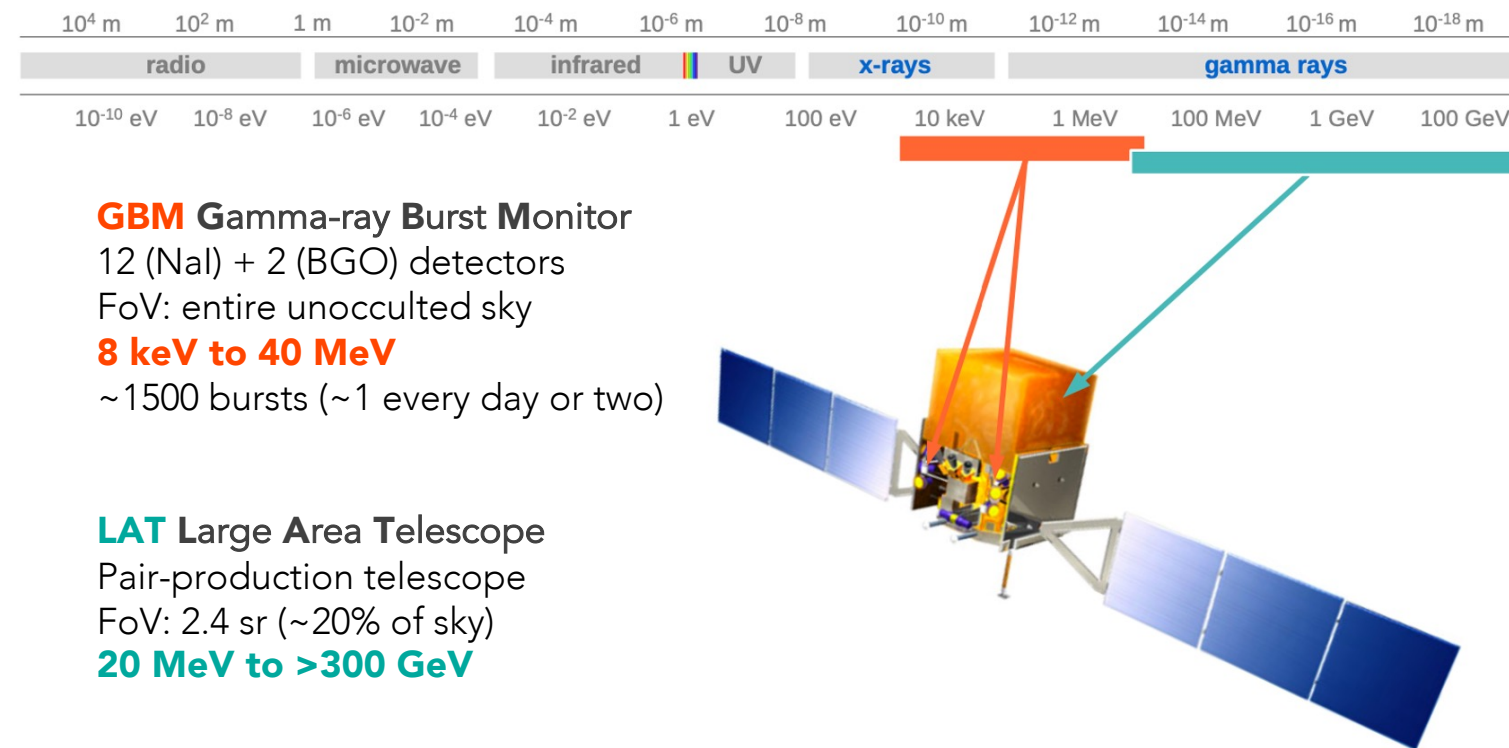
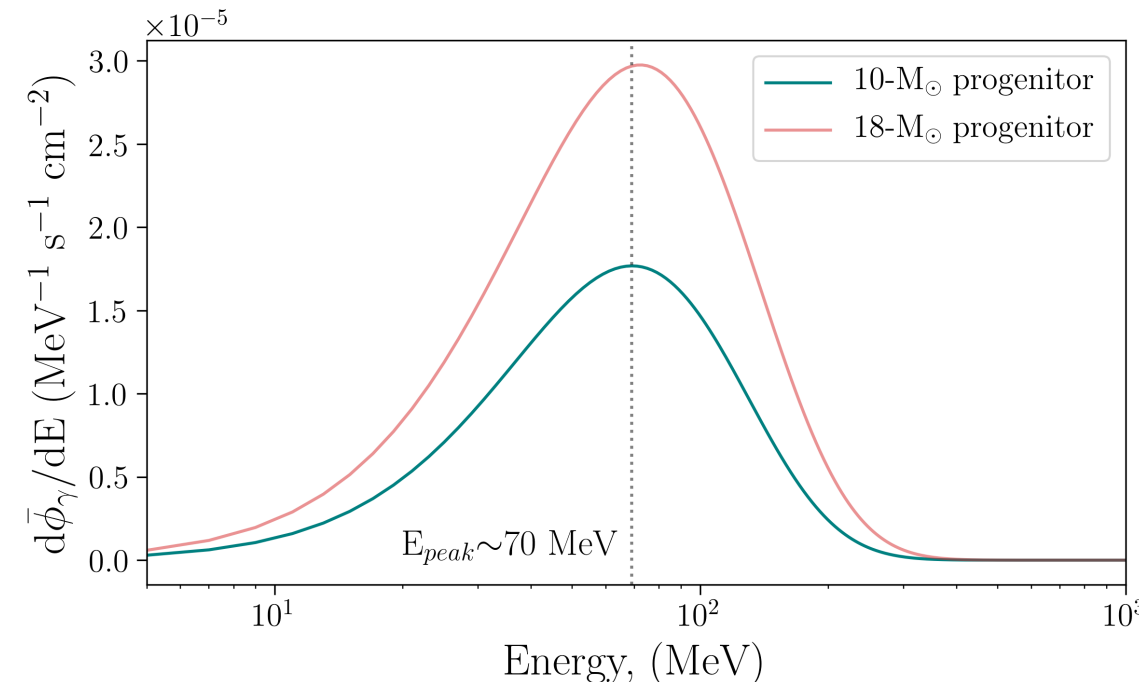
LAT Large Area Telescope

Pair-production telescope

FoV: 2.4 sr (~20% of sky)

20 MeV to >300 GeV

ALP spectrum



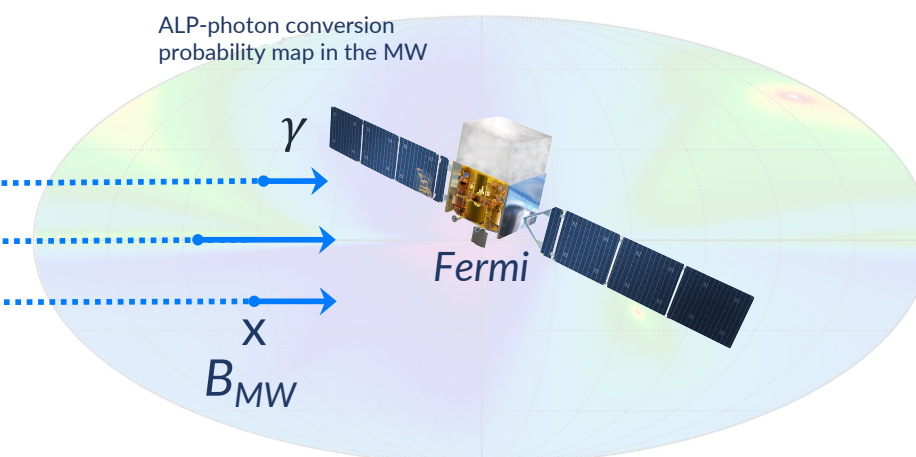
LAT low-energy technique (LLE)

- Standard LAT analysis: > 100 MeV (e.g. Meyer et al. 2020)
- LLE analysis: > 20 MeV
 - Maximizes the effective area of the LAT instrument in the low-energy regime
 - Relaxing requirements on the background rejection: **more signal, but also more background!**
 - Only works for pulse-like sources (i.e., transients)
 - Additional response functions needed (Monte Carlo simulations of a bright point source at the position of interest)
 - Systematics: flux values on average lower than those from the standard LAT analysis (see e.g. Ajello et al. 2014)

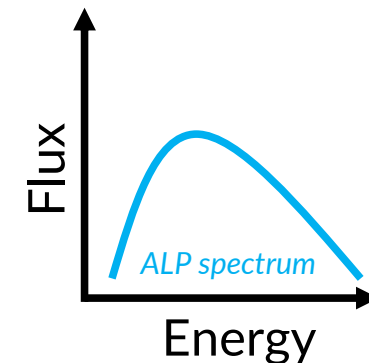
Motivation and assumptions



Primakoff
Process
inside the
CCSN core



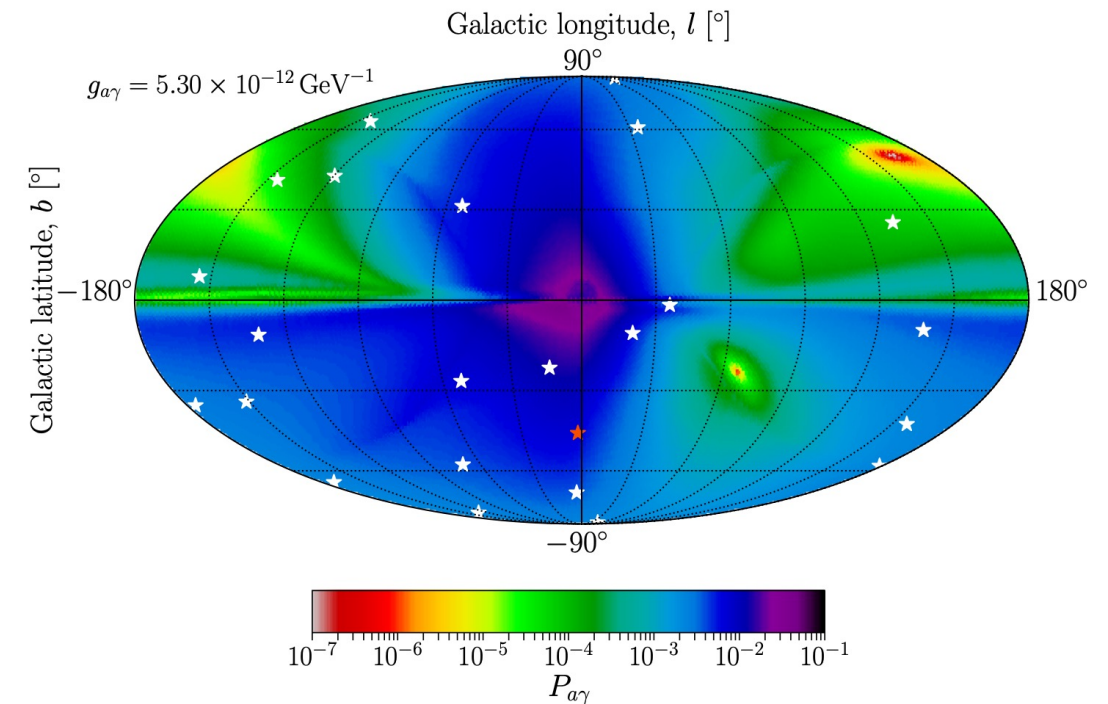
Inverse
Primakoff
Process
in the MW
B-field



► **Motivation:** ALPs are theorized to have a unique spectral signature in the spectrum of a long GRB. No other known physical processes are predicted to produce such signature.

Assumptions:

magnetic fields: only considering the MW magnetic field, neglecting IGMF



ALP-photon conversion probability map in the Milky Way's magnetic field.

Sensitivity testing: analysis and results

Model backgrounds from the considered LLE-detected GRB sample.

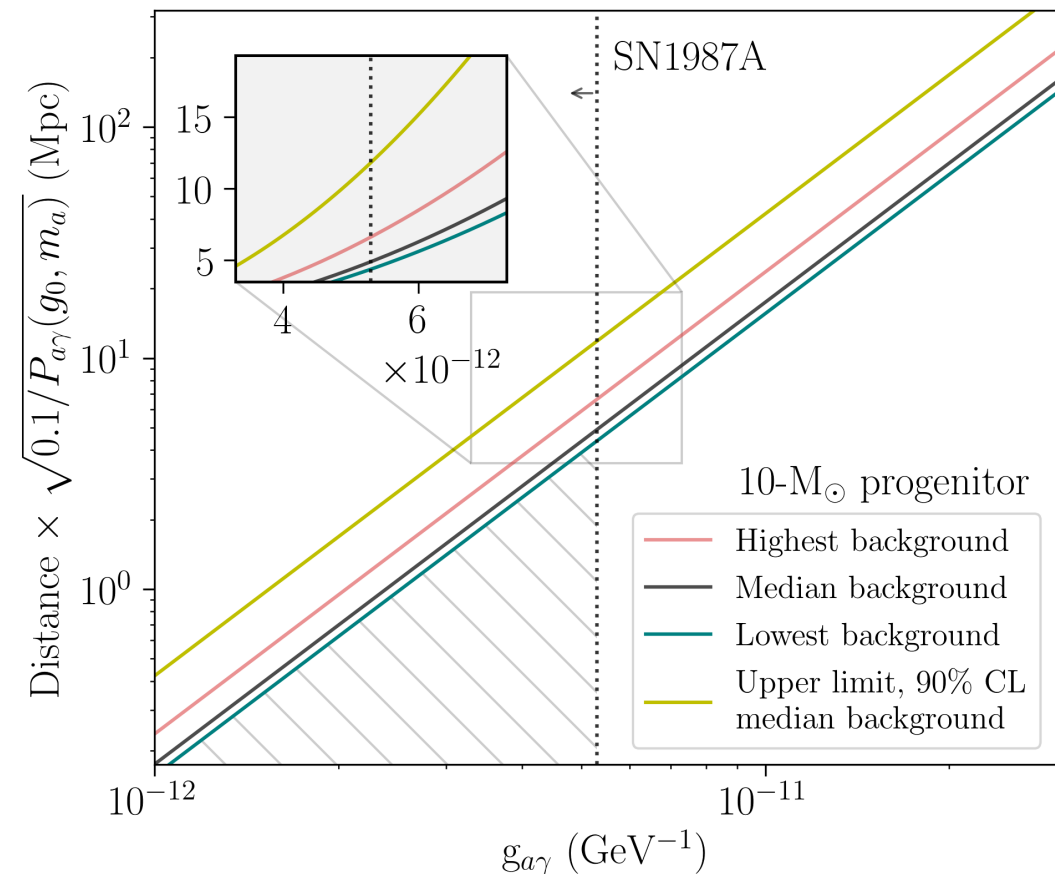
Find the min, max, and median background levels.

Produce ALP signal normalized by a value from the normalization grid for 10-and 18-solar-mass progenitors.

Produce 2000 realizations of the background+ALP spectrum and their corresponding (GRB) response functions (XSPEC fakeit function.)

Fit the ALP and the “background-only” model. Apply Wilks’ Theorem and LLR test to find for which normalization ALP model is preferred ($N_{\text{ALP}} \propto \frac{g_{a\gamma}^4}{d^2}$).

Find the coupling-distance parameter space for that normalization.



Conversion probability	Distance limit (Mpc)		
	Background level:		
$P_\gamma(g_0)$	Low	Median	High
0.1	4.4 (6.5)	4.9 (7.1)	6.6 (9.7)
0.05	3.1 (4.6)	3.5 (5.0)	4.7 (6.9)
0.01	1.4 (2.1)	1.5 (2.3)	2.1 (3.1)
0.001	0.4 (0.7)	0.5 (0.7)	0.7 (1.0)

Sensitivity testing: analysis and results

Model backgrounds from the considered LLE-detected GRB sample.

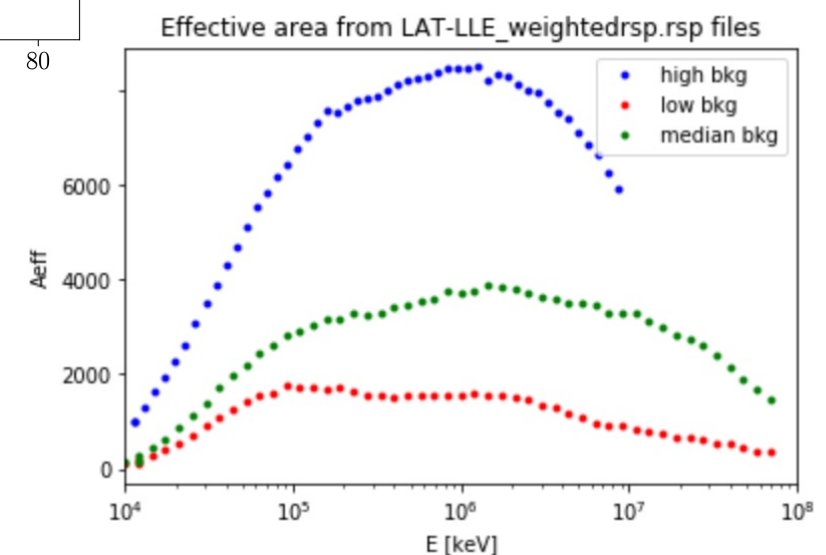
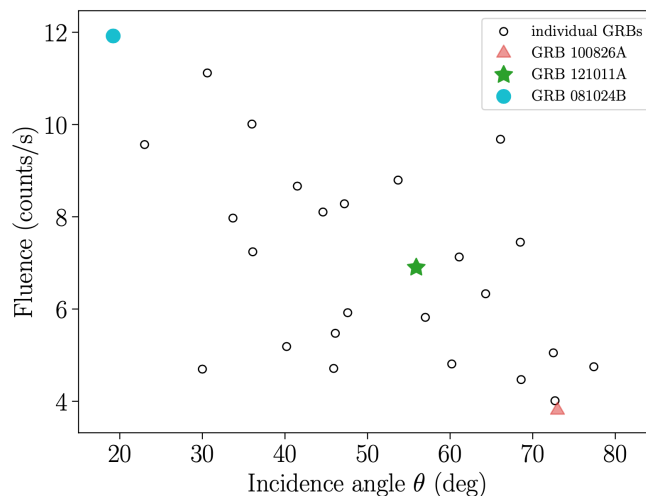
Find the min, max, and median background levels.

Produce ALP signal normalized by a value from the normalization grid for 10-and 18-solar-mass progenitors.

Produce 2000 realizations of the background+ALP spectrum and their corresponding (GRB) response functions (XSPEC fakeit function.)

Fit the ALP and the “background-only” model. Apply Wilks’ Theorem and LLR test to find for which normalization ALP model is preferred ($N_{\text{ALP}} \propto \frac{g_{a\gamma}^4}{d^2}$).

Find the coupling-distance parameter space for that normalization.



$P_\gamma(g_0)$	Conversion probability			Distance limit (Mpc)		
				Background level:		
				Low	Median	High
0.1				4.4 (6.5)	4.9 (7.1)	6.6 (9.7)
0.05				3.1 (4.6)	3.5 (5.0)	4.7 (6.9)
0.01				1.4 (2.1)	1.5 (2.3)	2.1 (3.1)
0.001				0.4 (0.7)	0.5 (0.7)	0.7 (1.0)

GRB Analysis Results

Property	Selection Criterion
Distance	unassociated (no redshift)
Detection significance	$\geq 5\sigma$ in LAT-LLE ($\gtrsim 30$ MeV)
Observed time interval	\geq duration of the burst
Burst duration	long GRBs ($T_{95} \gtrsim 2$ seconds) <i>(not used in Sec. IV)</i>

Initial sample: 186 LAT-detected GRBs

Applying the selection criteria

24 GRBs

GRB Analysis Results

GRB	T ₉₅ (s)	Best model(no ALP)	grbm parameters				LLR
			α_1	α_2	E_c (keV)		
080825C	22.2	grbm	-0.65 ^{+0.05} _{-0.05}	-2.41 ^{+0.04} _{-0.04}	143 ⁺¹³ ₋₁₂	0.2	
090217	34.1	grbm	-1.11 ^{+0.04} _{-0.04}	-2.43 ^{+0.03} _{-0.04}	16 ⁺¹³ ₋₈	0.1	
100225A	12.7	grbm	-0.50 ^{+0.25} _{-0.21}	-2.28 ^{+0.07} _{-0.09}	223 ⁺¹¹² ₋₆₈	0.0	
100826A	93.7	grbm+bb	-1.02 ^{+0.04} _{-0.04}	-2.30 ^{+0.03} _{-0.04}	484 ⁺⁷² ₋₆₃	0.0	
101123A	145.4	grbm+cutoffpl	-1.00 ^{+0.07} _{-0.08}	-1.94 ^{+0.15} _{-0.12}	187 ⁺⁷⁴ ₋₆₂	5.8	
110721A	21.8	grbm+bb	-1.24 ^{+0.02} _{-0.01}	-2.29 ^{+0.03} _{-0.03}	1000 ⁺²⁸ ₋₃₉	0.0	
120328B	33.5	grbm+cutoffpl	-0.67 ^{+0.06} _{-0.05}	-2.26 ^{+0.05} _{-0.05}	101 ⁺¹² ₋₁₃	0.0	
120911B	69.0	grbm	-2.50 ^{+0.92} _{-1.04}	-1.05 ^{+0.63} _{-0.38}	11 ⁺¹⁰ ₋₂	0.0	
121011A	66.8	grbm	-1.08 ^{+0.10} _{-0.21}	-2.18 ^{+0.11} _{-0.16}	997 ⁺⁸⁴ ₋₂₆	0.0	
121225B	68.0	grbm	-2.38 ^{+1.02} _{-0.40}	-2.45 ^{+0.06} _{-0.07}	11 ⁺⁸⁹ ₋₃	0.0	
130305A	26.9	grbm	-0.76 ^{+0.03} _{-0.03}	-2.63 ^{+0.06} _{-0.06}	665 ⁺⁶¹ ₋₅₅	0.0	
131014A	4.2	grbm	-0.55 ^{+0.33} _{-0.98}	-2.65 ^{+0.17} _{-0.19}	255 ⁺³⁶ ₋₁₁	0.63	
131216A	19.3	grbm+cutoffpl	-0.46 ^{+0.28} _{-0.24}	-2.67 ^{+1.94} _{-0.94}	178 ⁺⁷⁷ ₋₉₂	0.0	
140102A	4.1	grbm+bb	-1.10 ^{+0.12} _{-0.09}	-2.41 ^{+0.16} _{-0.11}	206 ⁺⁶⁵ ₋₉₂	2.3	
140110A	9.2	grbm	-2.49 ^{+1.64} _{-1.59}	-2.19 ^{+0.20} _{-0.22}	11 ⁺²³ ₋₃	0.0	
141207A	22.3	grbm+bb	-1.21 ^{+0.09} _{-0.06}	-2.33 ^{+0.11} _{-0.13}	999 ⁺¹⁸ ₋₇₀	0.0	
141222A	2.8	grbm+pow	-1.57 ^{+0.03} _{-0.02}	-2.83 ^{+0.46} _{-1.74}	9971 ⁺³⁹⁰ ₋₈₃₂	0.0	
150210A	31.3	grbm+pow	-0.52 ^{+0.04} _{-0.05}	-2.91 ^{+0.11} _{-0.38}	1000 ⁺⁵¹⁷ ₋₂₃₄	0.0	
150416A	33.8	grbm	-1.18 ^{+0.04} _{-0.04}	-2.36 ^{+0.13} _{-0.21}	999 ⁺¹⁸⁷ ₋₂₆₉	0.0	
150820A	5.1	grbm	-0.99 ^{+0.56} _{-1.30}	-2.01 ^{+0.82} _{-0.27}	303 ⁺⁶¹ ₋₃₉	0.0	
151006A	95.0	grbm	-1.35 ^{+0.06} _{-0.03}	-2.24 ^{+0.07} _{-0.08}	998 ⁺³³ ₋₈₄	0.0	
160709A	5.4	grbm+cutoffpl	-1.44 ^{+0.18} _{-0.12}	-2.18 ^{+0.15} _{-0.18}	9940 ⁺³⁷³ ₋₅₁₁	1.0	
160917A	19.2	grbm+bb	-0.78 ^{+3.45} _{-1.40}	-2.39 ^{+0.20} _{-0.10}	994 ⁺⁶³⁴ ₋₂₁₆	0.9	
170115B	44.8	grbm	-0.80 ^{+0.02} _{-0.04}	-3.00 ^{+0.10} _{-0.07}	1000 ⁺²²⁶ ₋₁₀₆	2.8	

Summary

- We consider light ALPs, hypothetically produced in CCSNe, and converted into gamma-rays in the MW magnetic field
- We test LAT sensitivity, including the LLE data cut and extending into energies relevant to the ALP spectral signature (a few tens of MeV)
 - For a median background and representative ALP parameters (mass & coupling), LAT sensitivity to ALP signals from CCSNe are reached up to distances of up to ~ 10 Mpc
 - This result is driven by the dominating background in the LLE data & decreased effective area at high incidence angles
 - Good science case for future MeV instruments
- We conduct ALP fitting to the unassociated, long, LLE-detected GRBs. No statistically significant detection in our sample. Highly unlikely that the GRB trigger time is the same as the ALP emission time (most of the selected GRBs are well-fit by the common GRB models)

Currently:

- Re-examining our time windows for ALP detection: 100's of seconds prior to the GRB trigger time on an extended sample of GBM & LAT GRBs
- Crnogorčević et al. 2022 in prep. (to be submitted in <4 months)